# Inhibition of mammalian target of rapamycin (mTOR) improves neurobehavioral deficit and modulates inflammatory response after traumatic brain injury

**Irene Paterniti**
Universita degli Studi di Messina
**Michela Campolo**
Universita degli Studi di Messina
**Giovanna Casili**
Universita degli Studi di Messina
**Marika Lanza**
Universita degli Studi di Messina
**Alessia Filippone**
Universita degli Studi di Messina
**Marika Cordaro**
Universita degli Studi di Messina
**Alessio Ardizzone**
Universita degli Studi di Messina
**Sarah Scuderi**
Universita degli Studi di Messina
**Salvatore Cuzzocrea**
Universita degli Studi di Messina
**Emanuela Esposito** ( eesposito@unime.it )
Universita degli Studi di Messina

**Research**

**Keywords:** Traumatic brain injury, mTOR, neuroinflammation

**Posted Date:** February 20th, 2020

**DOI:** https://doi.org/10.21203/rs.2.24093/v1

# Abstract

Traumatic brain injury (TBI) induce primary and secondary damage on endothelium and brain parenchyma, leading neurons die rapidly by necrosis. The mammalian target of rapamycin signalling pathway (mTOR) mediates many aspects of cell growth and regeneration and is up-regulated after moderate to severe traumatic brain injury (TBI). The significance of this increased signalling event for recovery of brain function is presently unclear, here we used two different selective inhibitors of mTOR activity to explore the functional role of mTOR inhibition in an validated model of TBI, the controlled cortical impact injury (CCI). We treated animals withKU0063794, a dual mTORC1 and mTORC2 inhibitor, and with rapamycin a well-known inhibitor of mTOR, 1 and 4 hours after TBI. Our results demonstrated that mTOR inhibitors, especially KU0063794, significantly improve motor and cognitive recovery after TBI as well as reduce lesion volumes. Moreover we observed that mTOR inhibitors treatment ameliorate the neuroinflammation associated to TBI and showed that this acute treatment significantly diminished the extent of neuronal death, astrogliosis and apoptotic process after trauma. Our findings suggest that the neuronal mTORC1/2 activity after TBI is deleterious to brain function and acute intervention with selective mTORC1/2 inhibitor may represent an effective therapeutic strategy to improve recovery after brain trauma.


# Introduction

Traumatic brain injury (TBI) is a serious public health problem affecting several people worldwide.

Even mild, closed-head trauma to the brain can lead to temporary or permanent neurological symptoms, including epileptic seizures, behavioural changes, and impaired motor and cognitive function. It is worth mentioning that neurological, behavioural and cognitive deficits are well-known sequelae of TBI, which lead to long-term functional impairment and decrease in quality of life (1).

Brain damage can arise from a combination of direct neuronal tissue damage, that is the primary injury, to the inflammatory response and excitotoxic damage that initiates secondary injury. The secondary non mechanical damage is multiple inflammatory responses follow TBI characterized by microglial and astrocytes activation, resulting in the release of reactive oxygen species and pro-inflammatory cytokines (2–4). These responses may determine whether microglial cell activity leads to the clearance of tissue debris and subsequent resolution of the inflammatory response or leads to chronic inflammation. In addition, recent study identified in the initiation, progression, and completion of autophagy, mediated by phosphatidylinositol/protein kinase B Akt/mammalian target of rapamycin (PI3K/Akt/mTOR) pathway, an important role in brain responses associated to head trauma (5, 6). Autophagy is a major player in the control of cell size, dendrite and axon outgrowth during brain development, and repair (7, 8). Several key molecular components participate in the induction and progression of autophagy, like the mammalian target of rapamycin (mTOR) as well as Beclin 1 and LC3. Two mTOR complexes have been characterized, termed mTOR complex-1 (mTORC1) and mTOR complex-2 (mTORC2) that individually plays an essential role in the control of cell proliferation (9, 10). The mTORC1 stimulate protein synthesis by mRNA

translation and cell development by entering the G1 phase of the cell cycle; however, mTORC2, firstly identified as a regulator of the actin cytoskeleton, has also been indicated to phosphorylate members of the AGC kinase family, including Akt, which is linked to several pathological conditions. They have distinctive downstream targets, different biological functions and importantly, different sensitivity to the drug rapamycin. Growth factors and hormones typically stimulate this pathway through the activation of receptor tyrosine kinases, leading to the activation of the PI3K and downstream Akt, which in turn regulates the activity of many signalling molecules, including mTOR. mTORC1 activation specifically induces protein translation through activation of ribosomal protein S6 kinases and disinhibition of the transcription initiation factor eIF4E that is required to power cell growth and proliferation (11).

Our previous study demonstrated that inhibition of mTOR produced a neuroprotective effect in an in vivo model of spinal cord injury (SCI), in which the inflammatory response is the key contributor of expansion of the lesion and further loss of neurologic function (12).

Moreover, it has been demonstrated that inhibition of mTORC1 pathway mediated by treatment with rapamycin, has protective effects in animal models of TBI in terms of behavioural performance measured by extent of tissue damage, motor function and neurological score (13, 14).

Despite different in vivo studies demonstrated the beneficial effects of Rapamycin on behavioral performance, however, limitations for its use in the human patient population exist, since Rapamycin produce considerable side effects, especially when treatment is prolonged.

Thus, based on these observations, in this study we hypothesized to investigated a new second generation of mTOR inhibitor, such as KU0063794, in an animal model of TBI, compared with a well know and characterized mTOR inhibitor Rapamycin .

KU0063794 is known to confer specific inhibition not only on mTORC1 but also on the other kinase complexes, such as mTORC2, suggesting that inhibition of both may be a viable strategy to ameliorate several aspects of functional recovery after TBI.

## Methods

# Animals

Male CD1 mice (25–30 g, Envigo, Italy), aged between 10 and 12 weeks, were used for all studies. Mice were placed in a controlled location with standard rodent chow and water. Animals were kept at 22 ± 1 °C with a 12-h light, 12-h dark cycle. The study was permitted by the University of Messina Review Board for the care of animals. All animal experiments were performed following the regulations in Italy (D.M. 116192), Europe (O.J. of E.C. L 358/1 12/18/1986).

# Controlled Cortical Impact (CCI) Experimental TBI

Mice were anesthetized with intraperitoneal (i.p.) administration of ketamine and xylazine (2.6 and 0.16 mg/kg body weight, respectively). TBI was induced in mice by a controlled cortical impactor (CCI) as previously described (15). In brief, a craniotomy was made in the right hemisphere, encompassing bregma and lambda, and between the sagittal suture and the coronal ridge, with a Micro motor hand piece and drill. The resulting bone flap was removed, and the craniotomy enlarged further. A cortical contusion was produced on the exposed cortex using the controlled impactor device Impact OneTM Stereotaxic impactor for CCI (Leica, Milan, Italy), the impact tip was centered and lowered over the craniotomy site until it touched the dura mater. Then, the rod was retracted, and the impact tip was advanced farther to produce a brain injury of moderate severity for mice (tip diameter: 4 mm; cortical contusion depth: 3 mm; impact velocity: 1.5 m/s). Immediately after injury, the skin incision was closed with nylon sutures, and 2% lidocaine jelly was applied to the lesion site to minimize any possible discomfort.

# Experimental design

Mice were randomly allocated into the following groups:

Sham + vehicle: mice were subjected to the surgical procedures except that the impact tip was not applied, and vehicle dimethyl sulfoxide (DMSO), was administered at 1 after craniotomy (n = 20);

TBI + vehicle: mice were subjected to CCI and vehicle (DMSO) was administered at 1 after craniotomy(n = 20);

TBI + Rapamycin (1 mg/kg): mice were subjected to CCI and Rapamycin (1 mg/kg in 10% DMSO) was administered orally 1 h and 4 h after craniotomy(n = 20);

TBI + KU0063794 (1 mg/kg): mice were subjected to CCI and KU0063794 (1 mg/kg in 10% DMSO) was administered intraperitoneally i.p. 1 h and 4 h after craniotomy (n = 20).

Sham + Rapamycin (1 mg/kg): mice were subjected to the surgical procedures as above group (anaesthesia and craniotomy) except that the impact tip was not applied and Rapamycin (1 mg/kg) was administered at 1 after craniotomy(n = 20).

Sham + KU0063794 (1 mg/kg): mice were subjected to the surgical procedures as above group (anaesthesia and craniotomy) except that the impact tip was not applied and KU0063794 (1 mg/kg) was administered at 1 after craniotomy(n = 20).

As describe below mice (n = 20 from each group and 10 for each technique) were sacrificed at 24 h after TBI to evaluate the various parameters.

# Behavioural testing

In another set of experiment, all animals were subjected to behavioural tests. All behavioural testing was conducted during the light cycle phase and in enclosed behaviour rooms (50–55 dB ambient noise)

within the housing room. The mice were placed in behaviour rooms 5 min for 2 days for acclimation prior to the onset of behavioural testing.

The behavioural tests were conducted by three different reliable expert observers blinded to the injury status of the animals. Tests are described below:

Rotarod test

The rotarod treadmill (Accuscan, Inc., Columbus, OH, USA) provided a motor balance and coordination assessment. This test was performed as previously described (16). Each animal was placed in a neutral position on a cylinder (1 cm diameter for mice), then the rod was rotated with the speed accelerated linearly from 0 to 24 rpm within 60 s, and the time spent on the rotarod was recorded automatically. The maximum score given to an animal was fixed to 60. For testing, animals were given three trials and the average score was used as the individual rotarod score.

Elevated Biased Swing Test

The EBST provided a motor asymmetry parameter and involved handling the animal by its tail and recording the direction of the biased body swings. The EBST consisted of 20 trials with the number of swings ipsilateral and contralateral to the injured hemisphere recorded and expressed in percentage to determine the biased swing activity. This analysis was performed as previous described (16).

# Tissue processing and histology

A qualified histopathologist evaluated coronal sections of 7-µm thickness from the perilesional brain area of each animal. Damaged neurons were counted and the histopathologic changes of the gray matter were scored on a six-point scale (22): 0, no lesion observed; 1, gray matter contained one to five eosinophilic neurons; 2, gray matter contained five to 10 eosinophilic neurons; 3, gray matter contained more than 10 eosinophilic neurons; 4, small infarction (less than one third of the gray matter area); 5, moderate infarction (one third to one half of the gray matter area); 6, large infarction (more than half of the gray matter area). The scores from all the sections of each brain were averaged to give a final score for individual mice. All the histological studies were performed in a blinded fashion.

# Quantification of lesion volume

The animals were anesthetized with ketamine, decapitated and their brains carefully removed. The brains were cut into 5 coronal slices of 2 mm thickness by using a McIlwain tissue chopper (Campdem instruments LTD). Slices were incubated in 2% solution of 2,3,5- triphenyltetrazolium chloride (TTC) (Sigma-Aldrich, Saint Louis, Missouri, USA) in Phosphate-buffered (0.1 mol/l) saline (PBS; pH 7.4) at 37 °C for 30 min and immersion fixed in 10% buffered formalin solution. Infracted area and volume was calculated from digital images (Canon 4×, Canon Inc., China) and ImageJ software 36. To account for brain edema, the lesioned areas were corrected by subtracting the area of the contralateral hemisphere area from the ipsilateral hemisphere 37. The corrected total lesion volume was estimated by summing

the lesioned area in every slice and multiplying it by slice thickness (2 mm). Lesion volume and area were measured on coronal brain slices for a total of three slices per animal.

# Immunohistochemistry

Tissue segments containing the lesion (1 cm on each side of the lesion) were fixed in 10% (w/v) buffered formaldehyde 24 h after TBI and sliced in 7-µm sections for paraffin-embedding previously described (15). After deparaffinization, endogenous peroxidase was quenched with 0.30% (v/v) hydrogen peroxide in 60% (v/v) methanol for 30 min. The sections were permeabilized with 0.1% (w/v) Triton X-100 in PBS for 20 min. Non-specific adsorption was minimized by incubating the section in 2% (v/v) normal goat serum in PBS for 20 min. Endogenous biotin or avidin binding sites were blocked by sequential incubation for 15 min with biotin and avidin, respectively. Afterwards, the sections were incubated overnight with one of the following primary antibodies diluted in PBS: anti-GFAP (1:500, Santa Cruz Biotechnology sc: 33673), anti-IBA1 (1:500, Santa Cruz Biotechnology sc:32725), anti-TNF-α (1:500, Santa Cruz Biotechnology sc-52746), anti-IL1β (1:500, Santa Cruz Biotechnology sc:32294), anti-Bax (1:500, Santa Cruz Biotechnology sc:526), anti-Bcl2 (1:500, Santa Cruz Biotechnology sc:492).

The immunohistochemical images were collected by Zeiss microscope using Axio Vision software. For graphic representation of densitometric analyses, we measured the intensity of positive staining (brown staining) by computer-assisted color image analysis (Leica QWin V3, UK). The percentage area of immunoreactivity (determined by the number of positive pixels) was expressed as percent of total tissue area (red staining) as seen previously (17).

# Western blot analyses for IkB-α, NF-κBp65, COX-2 and iNOS

Western blot was performed on tissue harvested 24 h post-TBI. Cytosolic and nuclear extracts were prepared as described previously (18). The filters were probed with specific Abs: anti- NF-κBp65 (1:500; Santa Cruz Biotechnology sc:8008), anti iNOS (1:500; Santa Cruz Biotechnology sc:8310), anti IκB-a (1:500; Santa Cruz Biotechnology sc:1643), anti-COX2 (1:500; Santa Cruz Biotechnology sc-1746), in 1 × PBS, 5% w/v non fat dried milk, 0.1% Tween-20 at 4 °C, overnight. To ascertain that blots were loaded with equal amounts of proteins they were also incubated in the presence of the antibody against β-actin protein (cytosolic fraction 1:500; Santa Cruz Biotechnology sc:8432) or lamin A/C (nuclear fraction 1:500 Sigma–Aldrich Corp.). Signals were detected with enhanced chemiluminescence (ECL) detection system reagent according to the manufacturer's instructions (Thermo, USA). The relative expression of the protein bands was quantified by densitometry with BIORAD ChemiDocTMXRS + software and standardized to β-actin and lamin A/C levels. Images of blot signals (8 bit/600 dpi resolution) were imported to analysis software (Image Quant TL,v2003).

# Immunofluorescence staining

After deparaffinization and rehydration, detection of NEU-N was carried out after boiling in 0.1 M citrate buffer for one minute as described previously (18). Non-specific adsorption was minimized by incubating the section in 2% (volume/ volume (vol/vol)) normal goat serum in PBS for 20 minutes. Sections were

incubated with mouse anti-Neun-N (1:100, vol/vol EMD Millipore) antibody in a humidified oxygen and nitrogen chamber for over night at 37 °C. Sections were incubated with secondary antibody Fluorescein isothiocyanate (FITC)-conjugated anti-mouse Alexa Fluor-488 antibody (1:2,000 vol/vol Molecular Probes, Monza, Italy) for one hour at 37 °C. For nuclear staining, 2 μg/ml 4',6'-diamidino-2-phenylindole (DAPI; Hoechst, Frankfurt, Germany) in PBS was added. To verify the binding specificity for used antibodies, control slices were incubated with only primary antibody or secondary antibody. In these controls no positive staining was detected Sections were observed at 20X magnification using a Leica DM2000 microscope (Leica, Milan, Italy). Optical sections of fluorescence specimens were obtained using a HeNe laser (543 nm), an ultraviolet laser (361 to 365 nm) and an argon laser (458 nm) at a one-minute, two seconds scanning speed with up to eight averages; 1.5 μm sections were obtained using a pinhole of 250. Contrast and brightness were established by examining the most brightly labeled pixels and applying settings that allowed clear visualization of structural details, while keeping the highest pixel intensities close to 200. The same settings were used for all images obtained from the other samples that had been processed in parallel. Digital images were cropped and figure montages prepared using Adobe Photoshop 7.0 (Adobe Systems; Palo Alto, California, United States). Cell counting analysis was made on rostro-caudal brain slices for a total of three slices per animal (n = 10 for each group).

# Materials

Rapamycin and KU0063794 was obtained by Tocris Bioscience (98%). All other chemicals were of the highest commercial grade available. All stock solutions were made in non-pyrogenic saline (0.9% NaCl, Baxter, Milan, Italy) or 10% dimethyl sulfoxide (DMSO). Except otherwise stated, all compounds were obtained from Sigma-Aldrich Company Ltd(Milan, Italy). All stock solutions were prepared in nonpyrogenic saline (0.9% NaCl; Baxter,Italy) or 10% dimethyl sulfoxide.

# Statistical evaluation

All values in the figures and text are expressed as mean ± standard error of the mean (SEM) of N number of animals. In those experiments involving histology or immunohistochemistry, the pictures exhibited are representative of at least three experiments performed on different days. Results were analyzed by one-way ANOVA followed by a Bonferroni post-hoc test for multiple comparisons. A p-value < 0.05 was considered significant. For one-way ANOVA statistic test, a single “F” value indicated as variation between sample means/variation within the samples was shown.

## Results

# KU0063794 treatment reduced the severity of brain trauma and the infarct outcome

To evaluate the effects of mTOR inhibitors on brain infarctions in the TBI, we performed TTC staining. An increased necrotic tissue area was observed in TBI mice compared to sham group (Fig. 1A); while treatments with Rapamycin and KU0063794 significantly attenuated the lesion area (Fig. 1A) following

TBI. Furthermore, the infarction area and infarct volume were significantly reduced after treatment with KU0063794 (Fig. 1B and 1 C respectively).

Also, to consider the correlation between neurological deficit and motor function in the setting of TBI, we performed EBST and rotarod test. Mice subjected to CCI showed a range of impairments in locomotor tasks as showed in Fig. 1D and 1E. KU0063794 treatment more efficacy than Rapamycin group, improved latency compared to TBI group (Fig. 1D and E respectively).

# Neuronal injury examination after TBI

To evaluate the contusion areas after TBI, the sections obtained from each group were stained with hematoxylin and eosin (H&E) staining. Histological examination revealed a significant tissue disorganization and white matter alteration in the brain parenchyma of TBI mice compared to sham animals (Fig. 2A and B respectively, see histological score 2E). Indeed, KU0063794 treatment significantly decrease the severity of trauma more effectively than Rapamycin (Fig. 2C and D respectively, see histological score analysis 2E).

Moreover, to assess the pathological changes in existing neuronal populations after TBI, we performed the immunofluorescence staining for NeuN marker of mature neurons. We observed that after TBI there was a significant reduction in a number of NeuN-positive neurons (Fig. 3B, see cells count 3E); instead NeuN- positive neurons were increased in the Rapamycin treated group and even more with KU0063794 treatment (Fig. 3C and D respectively, see cells count 3E) comparable to sham group neuron density.

# KU0063794 modulates IκBα degradation and NF-κBp65 nuclear translocation after TBI

To better understand the role of neuroinflammation in the progression of TBI we evaluated the NF-κB pathway by western blot analysis. Our results showed a significant decrease of IκBα expression in mice subjected to TBI (Fig. 4B A,A1) compared to sham group (Fig. 4A,A1); while KU0063794 treatment, more than Rapamycin, restored TBI-induced IkB-α degradation (Fig. 4A,A1).

Moreover, NF-κBp65 nuclear translocation was significantly increased after TBI, compared with sham group (Fig. 4B,B1); instead KU0063794 treatment considerably decreased the levels of NF-κBp65 more effectively than Rapamycin (Fig. 4B,B1).

# KU0063794 and Rapamycin attenuates inflammatory response induced by astrogliosis and microgliosis

Thus to evaluate the anti-inflammatory and neuroprotective effect of KU0063794 and Rapamycin treatments, we performed immunohistochemistry staining for TNFα and IL-1β.

We demonstrated that both TNFα and IL-1β levels were significantly increased after TBI (Fig. 5B and F respectively, see densitometry analysis I and J respectively) compared to control group (Fig. 5A and E respectively, see densitometry analysis I and J respectively). Meanwhile, KU0063794 and Rapamycin treatments significantly attenuated TNFα (Fig. 5C and D respectively, see densitometry analysis I and J respectively) and IL-1β (Fig. 5G and H respectively, see densitometry analysis I and J respectively) production, stimulated by TBI-induced microgliosis, with a great trend of protection with KU0063794 treatment.

Microgliosis and astrogliosis, meant as astrocytes and microglia activation, are a key component of the pathological onset and progression of TBI. Thus we evaluated, by immunohistochemistry staining, the expression of Iba1 and GFAP, as a marker of microglial and astrocyte activation respectively. A substantial increase in GFAP and Iba1 expressions (Fig. 6B and F respectively, see densitometry analysis I and J) were found in mice subject to TBI compared to sham animal (Fig. 6A and E respectively, see densitometry analysis I and J respectively). Whereas astrogliosis and microgliosis were significantly attenuated by KU0063794 (Fig. 6D and H respectively, see densitometry analysis I and J respectively) and Rapamycin treatments (Fig. 6C and G respectively, see densitometry analysis I and J respectively), with an higher trend of protection was observed after KU0063794 treatment.

# KU0063794 and Rapamycin modulates COX2 and iNOS expression in the brain after TBI

ROS-induced lipid peroxidation is the most studied mechanism of oxidative damage in TBI. A major enzymatic pathways in lipid peroxidation involved activation of inducible nitric oxide (iNOS) and cyclooxygenase-2 (COX-2) that we evaluated by western blot analysis. A substantial increase in COX2 and iNOS expression was observed in the brain from mice obtained at 24 h after TBI (Fig. 7C,C1 and D,D1) while KU0063794 treatment significantly reduced both expression more then the treatment with Rapamycin (Fig. 7C,C1 and D,D1).

# Effects of KU0063794 and Rapamycin on apoptosis pathway in the brain after TBI

To test whether brain damage was associated with apoptosis, the role of Bax and Bcl-2, a pro and anti-apoptotic factors respectively, was investigated by immunohistochemical staining. The expression of Bax was substantially increased in the brain subjected to TBI (Fig. 8B, see densitometry analysis I) compared to control mice (Fig. 8A, see densitometry analysis I). On the contrary, KU0063794 and Rapamycin treatment prevented TBI-induced Bax expression (Fig. 8C and D; see densitometry analysis I). On the

contrary the levels of Bcl2 were prompt reduced after TBI (Fig. 8B and F; see densitometry analysis J) and treatments with KU0063794 and Rapamycin showed an increase in Bcl-2 positive staining (Fig. 8G and H respectively; see densitometry analysis J) with a greater protection by KU0063794 treatment more than Rapamycin.

# Discussion

Neuroinflammation and microglial activation are key secondary injury mechanisms that contribute to chronic neurodegeneration and loss of neurological function after TBI (19).

The secondary injury after TBI develops over the post-traumatic period and is the result of a combination of vasogenic and cytotoxic edema, including glutamate excitotoxicity, disturbance of ionic homeostasis, lipid peroxidation and release of inflammatory regulators (20–22).

The key to developed future neuroprotective treatments that target post-traumatic neuroinflammation and microglial activation is to minimize the detrimental and neurotoxic effects of neuroinflammation while promoting the beneficial and neurotrophic effects (23).

Several recent studies have revealed that phosphorylation of phosphatidylinositol 3-kinase (PI3K)–Akt–mTOR and its downstream targets (p70S6K, S6 and 4E-BP1) increased within 30 minutes of a moderate injury to the parietal cortex and lasted up to 24 hours, activation that occurs in glial cells as well as in neurons at later time point.

Previous work on TBI corroborate the role of the PI3K/Akt/mTOR pathway in recovery from TBI, in particular the inhibition of mTOR activation mediated by rapamycin, a potent immunosuppressant is beneficial for ameliorating TBI-associated symptoms, including epilepsy and adverse inflammatory responses. Autophagy may exacerbate the pathological manifestations of TBI (24, 25), likely due to aberrant clearance of healthy cells in addition to degenerating cells. A regulatory mechanism should be devised to enhance the therapeutic autophagy, while blocking its deleterious side effects.

However, the use of rapamycin has limitations and warrant caution in the interpretation of results; for instance, the drug is recognised to confer nonspecific inhibition of other kinase complexes, such as mTORC2 and generate substantial side effects especially when treatment is long-drawn-out.

Thus, considered that an early intervention post-TBI could suppress neuronal mTORC activation reducing not only neuronal damage but also prevent glial dysfunction at later stages, we performed a CCI model of TBI that reproduces motor deficits and neuron loss that are evinced after TBI and we evaluated a neuroprotective effects of highly specific small-molecule inhibitor of mTOR kinase Ku0063794.

Ku0063794 inhibits both mTORC1 and mTORC2 thought phosphorylation of S6K1 and 4E-BP1, which are downstream substrates of mTORC1, and Akt phosphorylation on Ser473, which is the target of mTORC2 (26). We supposed that the strategies to target both mTORC1 and mTORC2 may produce better

responses after TBI as well as we wonder that KU0063794, has less toxicity of Rapamycin and permit a clear interpretation of data.

Thus, in our work we evaluated the effect of Ku0063794 in the control of the inflammatory process associated to TBI, as in the activation of NF- κB pathway, in the modulation of astrogliosis and microgliosis as well as in the control of pro-inflammatory cytokines production.

The early phase of damage usually occurs within minutes or 24 h following impact and it is directly associated to tissue damage, neurological dysfunction attributed to rapid cell death resulted in extensive dendritic degeneration and synapse reduction. Histological evaluation demonstrated that treatment with Ku0063794 determinate a reduction of the lesion area and showed a minor morphological modification that are visible following TBI.

Moreover, to assess the neurodegeneration occurring at an early stage following TBI, we evaluated by immunofluorescence staining a marker of mature neurons NeuN.

We observed that the expression of NeuN in the cortex and in the hippocampus was significantly decreased in mice subject to TBI; whereas the treatment with rapamycin and more efficacy with KU0063794 increased the number of NeuN positive cells, confirming the beneficial effect of mTOR inhibition on the loss of neuronal cells.

Following TBI, the inflammatory condition is a typical response that occurs to the adult mammalian CNS. It is know that some inflammatory mediators are locally released after injury and interact to control the cellular changes that occur in TBI. In particular, reactive gliosis is initiated in the surrounding neural tissue and spreads along the edges of the wound by the proliferation and migration of glial cells, this extended microglial activation at the focal site of injury becomes detrimental over time (27). Microglia are rapidly activated increasing in cell numbers at the site of the insult and produce inflammatory mediators such as pro-inflammatory cytokines that leads to actiavtion of astroglial and neovascularisation at trauma sites. Thus to better recognise if the mTOR inhibition could modulate the inflammatory process involved in TBI we evaluated the role of mTOR inhibitors in the control of the inflammatory pathway NF-κB as well as in decreasing microglia and astrocytes activation.

Our results clearly demonstrated that rapamycin and significantly better KU0063794, reduced the translocation of NF-κB in to the nucleus, translocation that is considerably increased in TBI group. NF-κB activation during TBI and the consequent translocation in the nucleus determinate the activation and the production of inflammatory factors such as pro-inflammatory cytokines. Thus, treatment with mTOR inhibitors along with NF-κB modulation had the capacity to decrease the amount of inflammatory cytokines, such as TNF-α and IL1-β. Therefore, pro-inflammatory cytokines are synthesized and secreted by astrocytes and microglia; consequently we investigate the role of mTOR inhibition in modulating astrogliosis and microgliosis by immunostaining for GFAP and IBA1 respectively markers for astrocytes and microglia activation. Accordingly we observed that rapamycin and much more KU0063794 significantly reduced astrocytes and microglia activation.

Once secreted, these pro-inflammatory cytokines can bind specific receptors to increase the amount of iNOS and COX2, as well as they can act as molecular inducers of programmed cell death or apoptosis (28).

We evaluated that mTOR inhibition regulate the expression of iNOS and COX2 that are significantly increased after TBI.

Moreover, an ensuing event associated with inflammation after TBI is the secondary cell death process of apoptosis (29). It is generally recognised that one mechanism underlying apoptotic cell death in TBI is a shift in the balance between pro- and anti-apoptotic factors towards the expression of proteins that promote cell death (30). Therefore, in the present study we also observed the role of mTOR signalling on cell death through the modulation of pro- and anti-apoptotic factors such as BAX and Bcl2 and in particular we observed that the treatment with mTOR inhibitors significantly reduced BAX expression and restored Bcl2 levels as control levels.

Thus, various inflammatory mediators play a pivotal role in produces systemic tissue damage following acute TBI and limiting the influx of inflammatory cells to the site of injury is a valuable approach to modulate the extent and distribution of inflammatory factors expressed in the injured CNS. Moreover, identifying the signalling pathway that could sustain microglia preserving their regenerative function after injury versus the predominating inflammatory activity, will provide an homeostatic mechanisms in maintaining a healthy brain.

Thereby, here we identify that mTOR activation, in hippocampal neurons, drives to cognitive dysfunction, neuronal damage, widespread astrogliosis and microgliosis. In particular, early intervention with mTOR inhibitors is considerably beneficial to limit tissue damage and improve functional recovery; especially we defined that inhibition of both mTORC1 and mTORC2 resulted more efficacy in reducing microglia and macrophage activation and significantly improving brain function.

In conclusion, a fuller understanding of the above pathophysiological processes will undoubtedly help to develop early diagnosis and potential therapeutic strategies and decrease the mortality rate for the TBI patients.

# Declarations

### Ethics approval and consent to participate:

Not applicable

### Consent for publication

Not applicable

### Availability of data and materials

The datasets used and/or analysed during the current study are available from the corresponding author on reasonable request

### Competing interests

The authors declare that they have no competing interests


### Funding

This research did not receive any specific grant from funding the work


### Authors' contributions

SC and EE planned the experiments; IP and MC prepared the manuscript and analyzed the results; GC and ML performed experiments; MC and AF performed the histochemical; SC and AA performed biochemical analysis.


### Acknowledgements

Not applicable


# References


1. Hawthorne G, Gruen RL, Kaye AH. Traumatic brain injury and long-term quality of life: findings from an Australian study. J Neurotrauma. 2009;26(10):1623-33.
2. Leker RR, Shohami E, Constantini S. Experimental models of head trauma. Acta Neurochir Suppl. 2002;83:49-54.
3. Leker RR, Shohami E. Cerebral ischemia and trauma-different etiologies yet similar mechanisms: neuroprotective opportunities. Brain Res Brain Res Rev. 2002;39(1):55-73.
4. Abdul-Muneer PM, Chandra N, Haorah J. Interactions of oxidative stress and neurovascular inflammation in the pathogenesis of traumatic brain injury. Mol Neurobiol. 2015;51(3):966-79.
5. Don AS, Tsang CK, Kazdoba TM, D'Arcangelo G, Young W, Zheng XF. Targeting mTOR as a novel therapeutic strategy for traumatic CNS injuries. Drug Discov Today. 2012;17(15-16):861-8.
6. Zhou H, Huang S. The complexes of mammalian target of rapamycin. Curr Protein Pept Sci. 2010;11(6):409-24.
7. Fingar DC, Salama S, Tsou C, Harlow E, Blenis J. Mammalian cell size is controlled by mTOR and its downstream targets S6K1 and 4EBP1/eIF4E. Genes Dev. 2002;16(12):1472-87.
8. Gong R, Park CS, Abbassi NR, Tang SJ. Roles of glutamate receptors and the mammalian target of rapamycin (mTOR) signaling pathway in activity-dependent dendritic protein synthesis in hippocampal neurons. J Biol Chem. 2006;281(27):18802-15.

9. Lebrun-Julien F, Bachmann L, Norrmen C, Trotzmuller M, Kofeler H, Ruegg MA, et al. Balanced mTORC1 activity in oligodendrocytes is required for accurate CNS myelination. J Neurosci. 2014;34(25):8432-48.
10. Norrmen C, Figlia G, Lebrun-Julien F, Pereira JA, Trotzmuller M, Kofeler HC, et al. mTORC1 controls PNS myelination along the mTORC1-RXRgamma-SREBP-lipid biosynthesis axis in Schwann cells. Cell Rep. 2014;9(2):646-60.
11. Zeng Z, Zhang Y, Jiang W, He L, Qu H. Modulation of autophagy in traumatic brain injury. J Cell Physiol. 2020;235(3):1973-85.
12. Cordaro M, Paterniti I, Siracusa R, Impellizzeri D, Esposito E, Cuzzocrea S. KU0063794, a Dual mTORC1 and mTORC2 Inhibitor, Reduces Neural Tissue Damage and Locomotor Impairment After Spinal Cord Injury in Mice. Mol Neurobiol. 2017;54(4):2415-27.
13. Wu H, Lu D, Jiang H, Xiong Y, Qu C, Li B, et al. Simvastatin-mediated upregulation of VEGF and BDNF, activation of the PI3K/Akt pathway, and increase of neurogenesis are associated with therapeutic improvement after traumatic brain injury. J Neurotrauma. 2008;25(2):130-9.
14. Erlich S, Alexandrovich A, Shohami E, Pinkas-Kramarski R. Rapamycin is a neuroprotective treatment for traumatic brain injury. Neurobiol Dis. 2007;26(1):86-93.
15. Cuzzocrea S, Doyle T, Campolo M, Paterniti I, Esposito E, Farr SA, et al. Sphingosine 1-Phosphate Receptor Subtype 1 as a Therapeutic Target for Brain Trauma. J Neurotrauma. 2018;35(13):1452-66.
16. Casili G, Campolo M, Paterniti I, Lanza M, Filippone A, Cuzzocrea S, et al. Dimethyl Fumarate Attenuates Neuroinflammation and Neurobehavioral Deficits Induced by Experimental Traumatic Brain Injury. J Neurotrauma. 2018;35(13):1437-51.
17. Impellizzeri D, Campolo M, Bruschetta G, Crupi R, Cordaro M, Paterniti I, et al. Traumatic Brain Injury Leads to Development of Parkinson's Disease Related Pathology in Mice. Front Neurosci. 2016;10:458.
18. Cordaro M, Impellizzeri D, Paterniti I, Bruschetta G, Siracusa R, De Stefano D, et al. Neuroprotective Effects of Co-UltraPEALut on Secondary Inflammatory Process and Autophagy Involved in Traumatic Brain Injury. J Neurotrauma. 2016;33(1):132-46.
19. Hernandez-Ontiveros DG, Tajiri N, Acosta S, Giunta B, Tan J, Borlongan CV. Microglia activation as a biomarker for traumatic brain injury. Front Neurol. 2013;4:30.
20. Lozano D, Gonzales-Portillo GS, Acosta S, de la Pena I, Tajiri N, Kaneko Y, et al. Neuroinflammatory responses to traumatic brain injury: etiology, clinical consequences, and therapeutic opportunities. Neuropsychiatr Dis Treat. 2015;11:97-106.
21. Acosta SA, Tajiri N, Shinozuka K, Ishikawa H, Grimmig B, Diamond DM, et al. Long-term upregulation of inflammation and suppression of cell proliferation in the brain of adult rats exposed to traumatic brain injury using the controlled cortical impact model. PLoS One. 2013;8(1):e53376.
22. Acosta SA, Diamond DM, Wolfe S, Tajiri N, Shinozuka K, Ishikawa H, et al. Influence of post-traumatic stress disorder on neuroinflammation and cell proliferation in a rat model of traumatic brain injury. PLoS One. 2013;8(12):e81585.

23. Loane DJ, Faden AI. Neuroprotection for traumatic brain injury: translational challenges and emerging therapeutic strategies. Trends Pharmacol Sci. 2010;31(12):596-604.
24. Bigford GE, Alonso OF, Dietrich D, Keane RW. A novel protein complex in membrane rafts linking the NR2B glutamate receptor and autophagy is disrupted following traumatic brain injury. J Neurotrauma. 2009;26(5):703-20.
25. Luo CL, Li BX, Li QQ, Chen XP, Sun YX, Bao HJ, et al. Autophagy is involved in traumatic brain injury-induced cell death and contributes to functional outcome deficits in mice. Neuroscience. 2011;184:54-63.
26. Garcia-Martinez JM, Moran J, Clarke RG, Gray A, Cosulich SC, Chresta CM, et al. Ku-0063794 is a specific inhibitor of the mammalian target of rapamycin (mTOR). Biochem J. 2009;421(1):29-42.
27. Loane DJ, Byrnes KR. Role of microglia in neurotrauma. Neurotherapeutics. 2010;7(4):366-77.
28. Combs CK, Karlo JC, Kao SC, Landreth GE. beta-Amyloid stimulation of microglia and monocytes results in TNFalpha-dependent expression of inducible nitric oxide synthase and neuronal apoptosis. J Neurosci. 2001;21(4):1179-88.
29. Gugliandolo E, D'Amico R, Cordaro M, Fusco R, Siracusa R, Crupi R, et al. Neuroprotective Effect of Artesunate in Experimental Model of Traumatic Brain Injury. Front Neurol. 2018;9:590.
30. Kovesdi E, Czeiter E, Tamas A, Reglodi D, Szellar D, Pal J, et al. Rescuing neurons and glia: is inhibition of apoptosis useful? Prog Brain Res. 2007;161:81-95.

# Figures

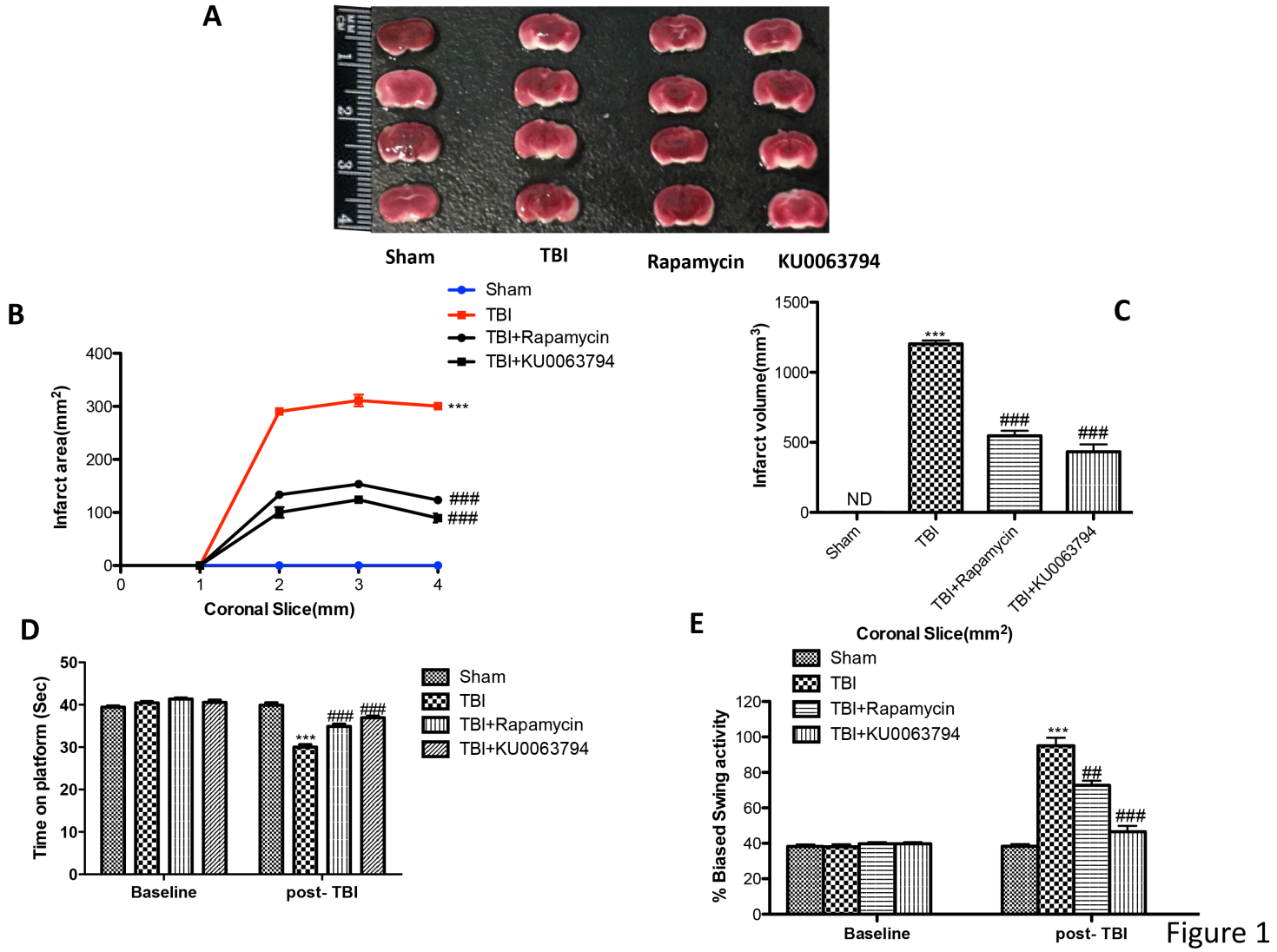


Figure 1

## Figure 2

Effect of mTOR inhibitors on brain infarction and on behavioral and neurological function following TBI. TTC staining (brick red) of coronal brain sections (2 mm thick) was performed 24 h after TBI. When compared to intense TTC staining in brains from sham-operated mice, brains from TBI mice had less TTC indicating greater levels of lesioned area (unstained regions) (A). Lesioned area (B) and volume (C) in rapamycin and KU0063794 treated mice were significantly reduced compared to TBI group. Moreover, TBI-injured mice showed significant impairments in motor deficits as revealed by shortened time to stay on rotarod (D) and augmented biased swing activity (E). On the contrary treatment with rapamycin and KU0063794significantly improved motor function (D and E). Data are means ± SEM of 10 mice for each group (three slices per animal). ***p< 0.001 vs. Sham; ## p< 0.01 vs. TBI; ###p< 0.001 vs. TBI.

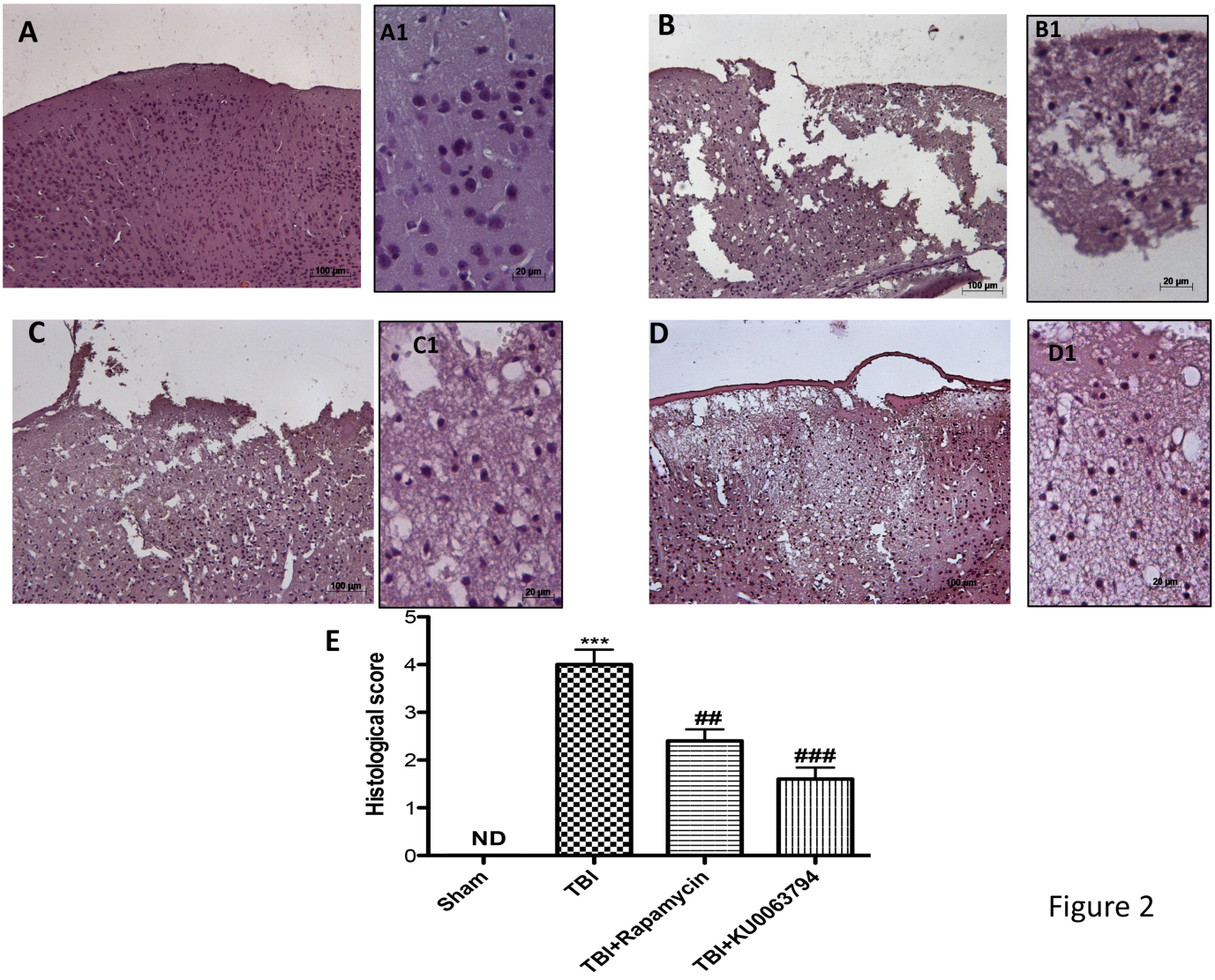


Figure 2

## Figure 4

Effects of Rapamycin and KU0063794 treatment on histological alterations after TBI A histological examination of brain sections showed tissue disorganization and cell infiltration in TBI injured mice (B and B1, see histological score E) respect to intact tissue structure observed in control mice (A and A1 , see histological score E). A significant protection from the TBI was apparent in Rapamycin and KU0063794 treated mice (C, C1 and D,D1, see histological score F). The figures are representative of at least three experiments performed on different experimental days. Data are means ± SEM of 10 mice for each group. One-Way ANOVA test ($p < 0.05$) followed by Bonferroni post-hoc test for multiple comparisons. ***$p < 0.001$ vs. Sham; ##$p < 0.001$ vs. TBI; ###$p < 0.001$ vs. TBI. ND, not detectable.

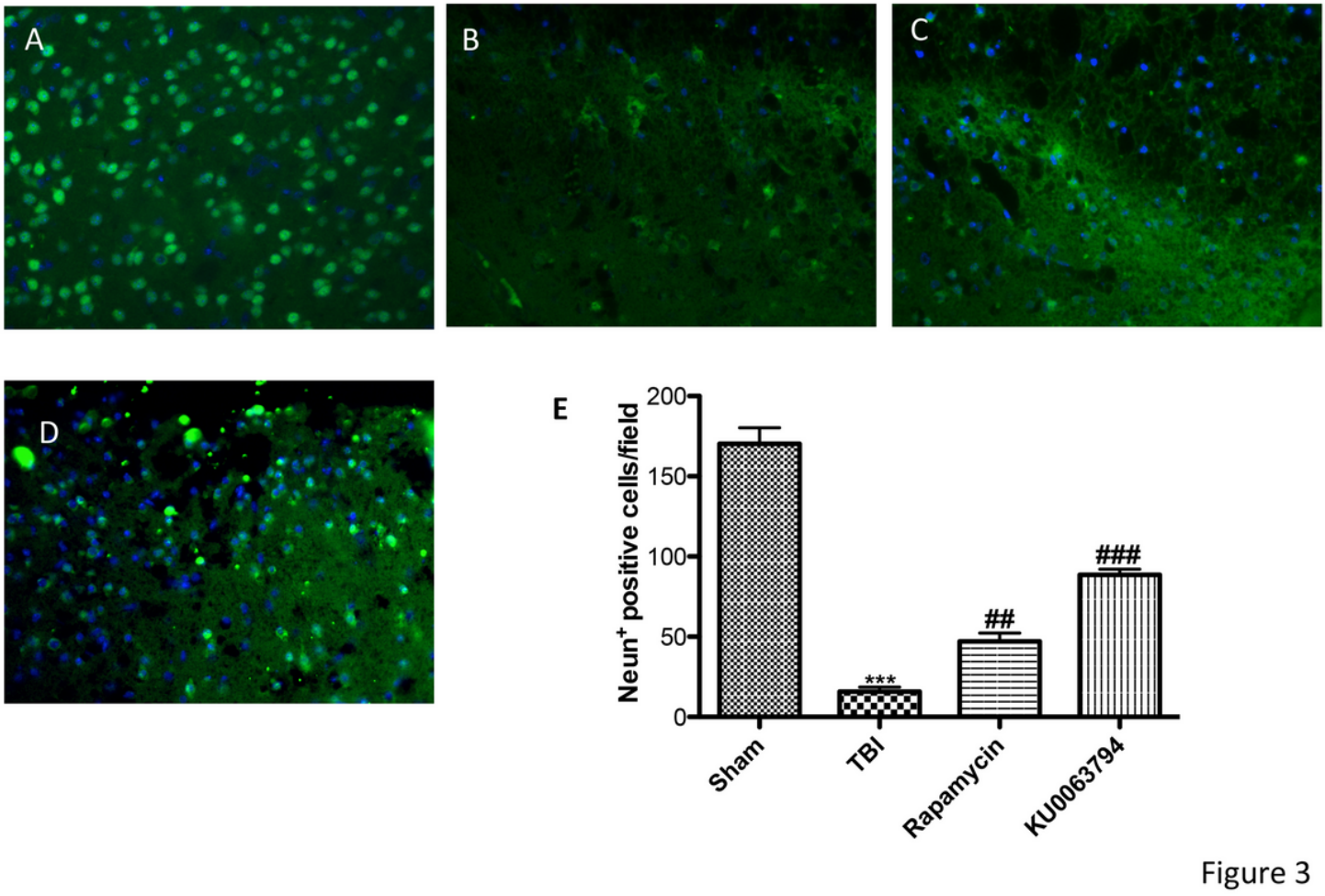


Figure 3

## Figure 6

Effects of mTOR inhibition on neuronal cells after TBI Representative images showing the intensity of fluorescent signals in regions labeled for NeuN and DAPI in the brain section from Sham animals (A, see cells count E), animals submitted to TBI (B, see cells count E), and animals treated with rapamycin (C,D, see cells count E). NeuN-positive neurons were significantly reduced after chronic TBI(B, see cells count E), while treatment with Rapamycin (C, see cells count E) and more significant KU0063794 (D, see cells count E) restored the number of neuronal cells. Each data are expressed as Mean ± SEM from N = 10 mice/group. Counting of colocalized cell confirmed our data. The co-localization of image was analysed with image J software.

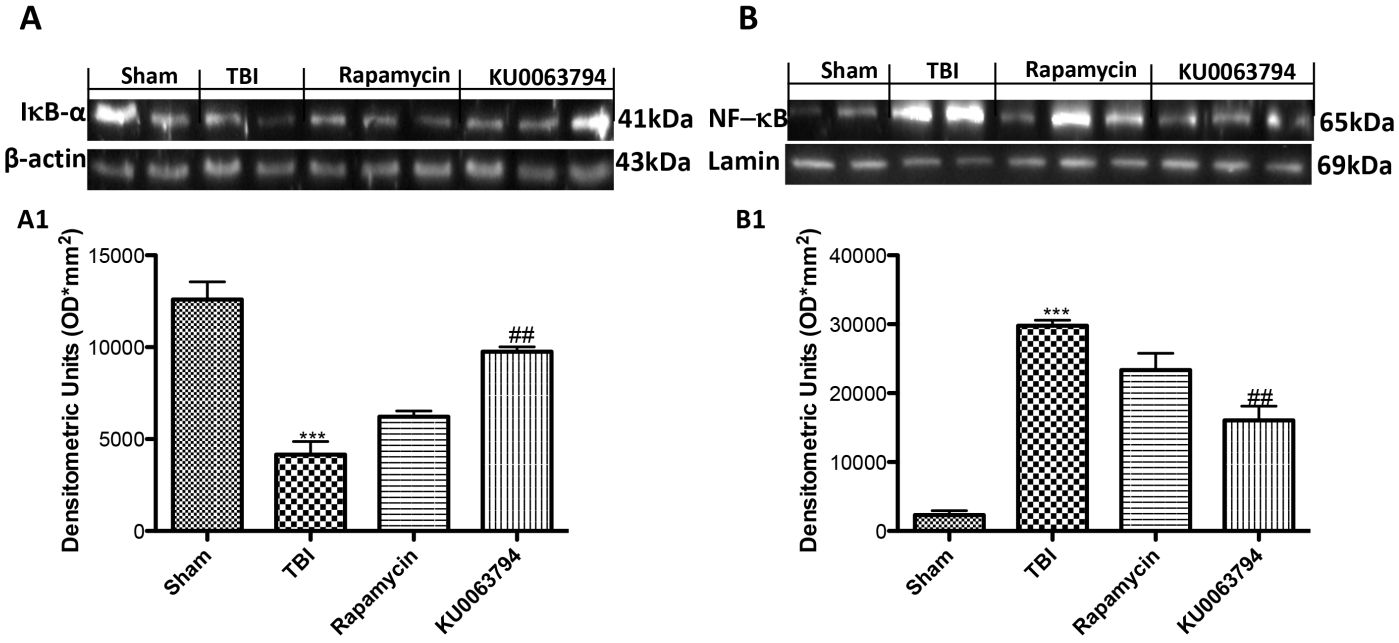


Figure 4

## Figure 8

Effects of chronic TBI on Nuclear factor κB (NF-κB) pathway and pro-inflammatory enzymes. Degradation of IκBα was significantly increased after TBI (A,A1). Also, TBI resulted in enhanced nuclear translocation of p65 (B,B1). Whereas Rapamycin and KU0063794 treatment significantly restored IκBα levels (A,A1) and reduced NF-κBp65 expression (B,B1). Data show one representative blot from three independent experiments with similar results. Data are expressed as Mean ± SEM from N = 10 mice/group. ***P < 0.005 vs. sham; ###p< 0.001 vs. TBI

## Figure 10

Effect of Rapamycin and KU0063794 on proinflammatory cytokines expression following TBI. When compared to sham, increased TNFα and IL-1β (B,D) expression was evident 24 h following TBI (B,B1 and F,F1 respectively, see densitometric analysis I and J). Administration of rapamycin attenuated the expression of both cytokines (C,C1 and G,G1 respectively, see densitometric analysis I and J). Moreover,

KU0063794 treatment significantly reduced TNFα (D,D1, see densitometric analysis I and J) and IL-1β expression (H,H1, see densitometric analysis I and J). The figures are representative of at least three experiments performed on different experimental days. Data are expressed as Mean ± SEM from N = 10 mice/group. One-Way ANOVA test (p< 0.05) followed by Bonferroni post-hoc test for multiple comparisons ***P < 0.001 vs. sham; ##p< 0.01 vs. TBI ###p< 0.001 vs. TBI. ND, not detectable.

## Figure 12

Effect of Rapamycin and KU0063794 on astrocytes and microglia activation following TBI. A remarkable increment in microglia and astrocytes activation was observed by immunostaining for GFAP and Iba1 respectively a markers for astrocytes and microglia activation. In TBI-injured animals there was a notably increment in the positive staining for both GFAP and Iba1(B,B1 and F,F1 respectively, see densitometric analysis I and J). Treatment with rapamycin and much more with KU0063794 reduced the activation of both astrocytes (C,C1 and G,G1 respectively, see densitometric analysis I and J) and microglia (D,D1 and H,H1 respectively, see densitometric analysis I and J). The figures are representative of at least three experiments performed on different experimental days Each data are expressed as mean ± SEM from n = 10 male One-Way ANOVA test (p< 0.05) followed by Bonferroni post-hoc test for multiple comparisons ***P < 0.001 vs. sham; ##p< 0.01 vs. TBI ###p< 0.001 vs. TBI. ND, not detectable.

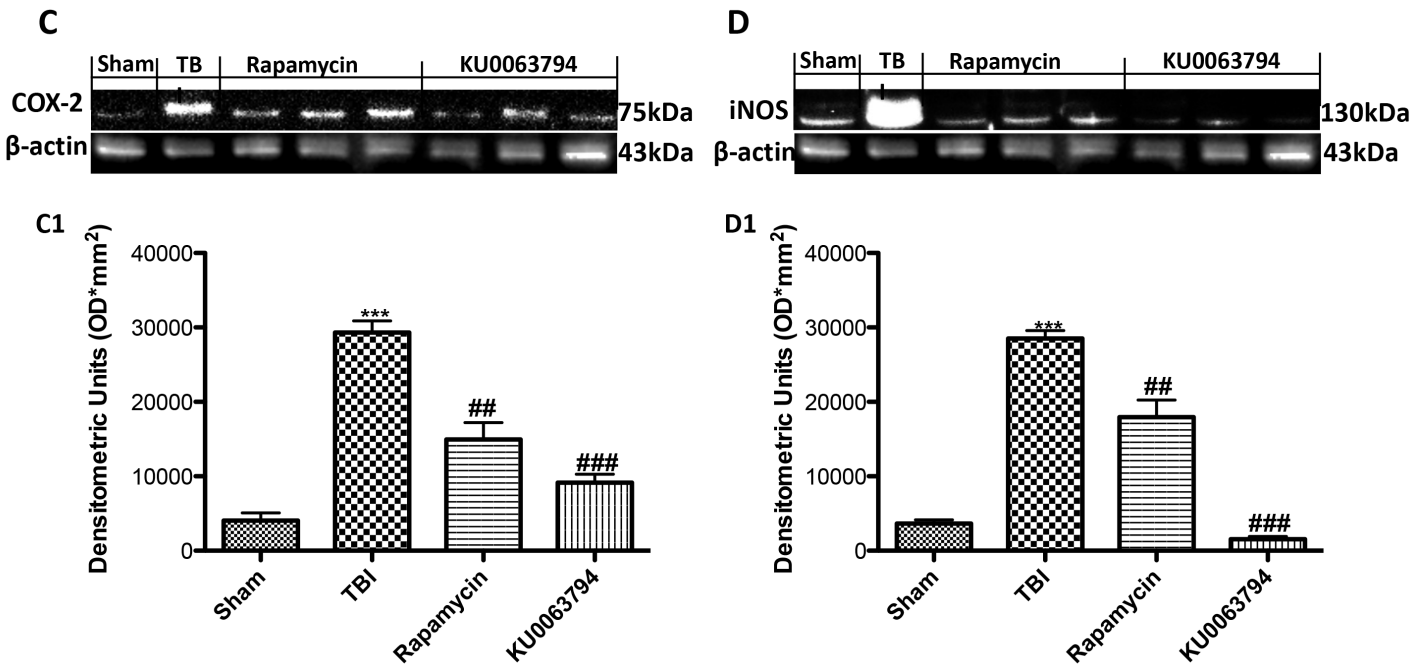


**Figure 7**

## Figure 14

Effects of mTOR inhibition on pro-inflammatory enzymes after TBI A significant increase in iNOS and COX2 was observed in the brain from TBI mice (A,A1 and B.B1 respectively) compared with the Sham mice (A,A1 and B.B1 respectively). Whereas Rapamycin and KU0063794 treatment significantly reduced iNOS and COX2 expression (A,A1 and B.B1 respectively). Data show one representative blot from three independent experiments with similar results. Data are expressed as Mean ± SEM from N = 10 mice/group. ***P < 0.005 vs. sham; ##p< 0.01 vs. TBI; ###p< 0.001 vs. TBI

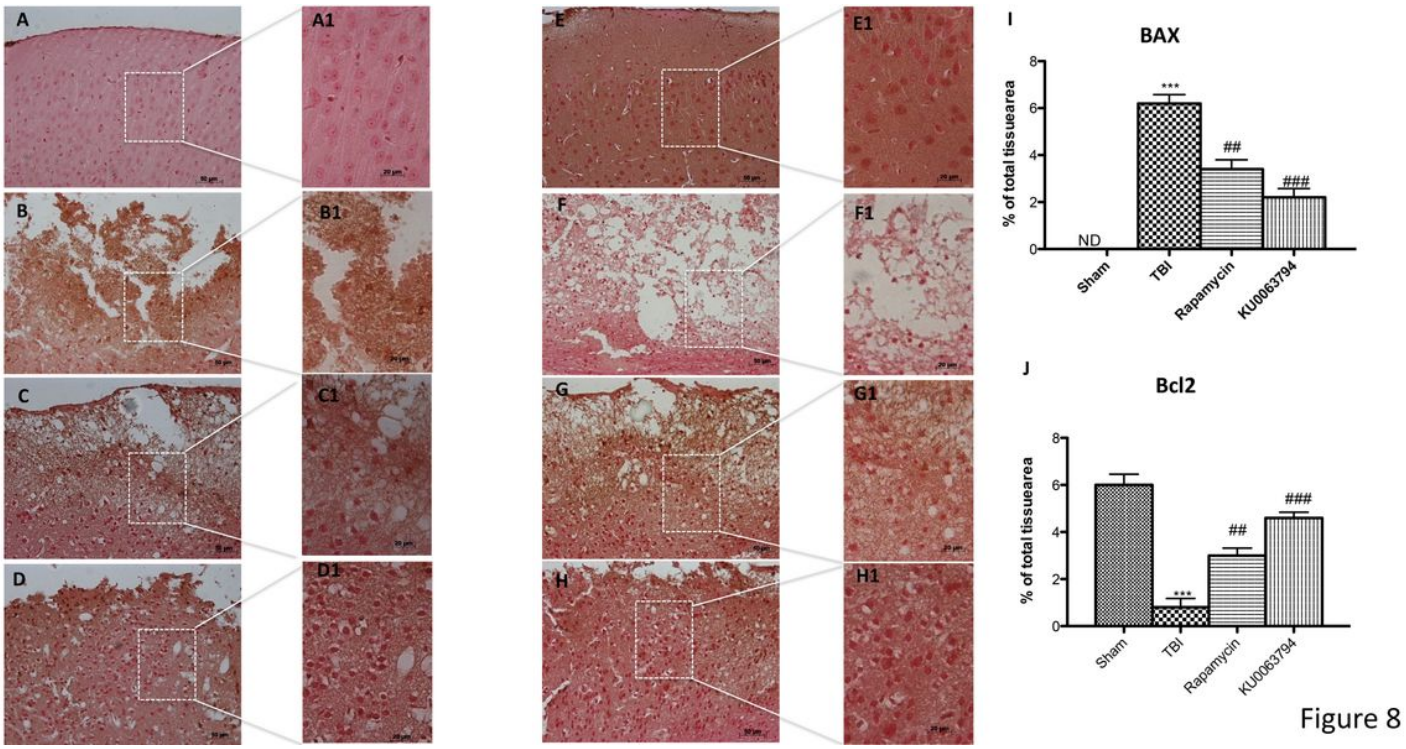


## Figure 16

Effects of Rapamycin and KU0063794 on apoptosis after TBI. At 24 h, an increase in Bax expression was observed in TBI-induced mice (B,B1, see densitometric analysis I). Treatment with rapamycin reduced the degree of positive staining and expression for Bax (C,C1, see densitometric analysis I), reduction that was more significantly with KU0063794 treatment (D,D1, see densitometric analysis I). On the contrary, positive staining for Bcl-2 was significantly reduced in TBI mice (F,F1, see densitometric analysis J), whereas rapamycin and KU0063794 treatment significantly restored Bcl2 staining (G,G1, and H,H1 see densitometric analysis J). The figures are representative of at least three experiments performed on different experimental days. Each data are expressed as Mean ± SEM from N=10 Mice for each group. One-Way ANOVA test ($p< 0.05$) followed by Bonferroni post-hoc test for multiple comparisons. ***$P < 0.005$ vs. sham; ##$p< 0.01$ vs. TBI; ###$p< 0.001$ vs. TBI